European Journal of Control 75 (2024) 100902

Contents lists available at ScienceDirect

European Journal of Control

journal homepage: www.elsevier.com/locate/ejcon

Optimizing restrictions in epidemics via piecewise time-varying SIRD models: Application to the COVID-19 Italian emergency

Alessandro Borri [a,*], Pasquale Palumbo [b,a], Federico Papa [a], Corrado Possieri [c,a]

[a] Institute for Systems Analysis and Computer Science "A. Ruberti", National Research Council of Italy (CNR-IASI), Rome, Italy
[b] Department of Biotechnology and Biosciences, University of Milano-Bicocca, Milan, Italy
[c] Department of Civil Engineering and Computer Science Engineering, University of Rome Tor Vergata, Rome, Italy

ARTICLE INFO

Article history:
Received 28 April 2023
Revised 11 August 2023
Accepted 26 August 2023

Recommended by Prof. T Parisini

Keywords:
Epidemic modeling
Predictive control
COVID-19
Receding-horizon optimization
Numerical simulation

ABSTRACT

The current coronavirus pandemic has produced severe consequences on economic and health systems all over the world, with the governments being challenged in searching for containment solutions balancing virus diffusion and limitations to social and work activities. In this paper, we propose a framework for the real-time optimization of restrictions in epidemics, based on the use of a time-varying SIRD model. Despite their simplicity, this class of models is able to capture the essential features of the epidemic spread, with the inherent parameter variation allowing accurate adaptation to real data. An optimization problem is formulated, properly balancing health and economic costs, and is solved parametrically by following a receding-horizon approach, resulting in an optimal sequence of social contact restrictions, which are assumed to be actuated via governmental containment measures. Numerical simulations based on the real data of the Italian COVID-19 emergency highlight the potential of the proposed approach and can be possibly helpful for the decision makers in present and future pandemics.

1. Introduction

At the beginning of 2020 the entire world has been found unprepared in facing the unprecedented sanitary emergency of the COVID-19 pandemic. The first cases of SARS-CoV-2 disease were notified in China, within the region of Wuhan. Due to the globalization, the infection spread along the Earth surface in less than one year, deeply affecting lives, social habits and the economies of all the countries, producing very rapidly the collapse of their health systems. After 16 months from the first diagnosed case, the COVID-19 pandemic caused the death of over 3.8 million people and the infection of more than 175 million of patients (without considering undiagnosed subjects) [40]. Such a large impact of the COVID-19 pandemic motivated a worldwide impressive research effort to understand its spread and the effectiveness of containment measurements [4,16,19,34].

The fast diffusion of COVID-19 pushed the governments of the entire world to rapidly adopt strong measures, like the lock-down and the limitations of social and economic activities, in addition to hygienic norms and face masks, in order to contain the disease spread. Such interventions, known as Non-Pharmaceutical Interventions (NPIs), proved to be very efficient to limit the disease diffusion and are the only weapons to stop the disease spread until specific drugs (against the virus and its complications) and efficient vaccines are available [15,35]. After 3 years, the epidemic scenario has changed but NPIs remain fundamental tools to be used even in the presence of vaccines since they have the fundamental role of limiting the virus circulation (and then its replication and the consequent mutations).

Despite this important role played by the NPIs in limiting the virus spread, such interventions (especially the limitations of social and economic contacts) have a strong impact on people lives, often implying a heavy economic and psychological burden [8,28,37,39]. For this reason, NPIs must be suitably planned and optimized in order to maximize their effects while minimizing their negative impact on the human lives. The planning and optimization of NPIs can be efficiently supported by mathematical models which are able to reproduce the infection mechanism and to predict the dynamical evolution of a given disease in the susceptible population.

* Corresponding author.
E-mail address: alessandro.borri@iasi.cnr.it (A. Borri).

https://doi.org/10.1016/j.ejcon.2023.100902

Recently, many papers addressing the mathematical description of COVID-19 and extending the basic SIR structure (Susceptible, Infected and Recovered) by McKendrick and Kermack [26], have been published. Multi-compartmental epidemic models have been formulated focusing on the mathematical representation of various aspects of the COVID-19: the presence of asymptomatic infection and of the incubation-latency period, the problem of the contagion tracking, the inclusion of quarantine and isolation compartments, the different severity levels of the disease etc. [9,12,13,18,20,21]. Such detailed representations of the disease have shown to provide realistic long term predictions and interesting quantitative analyses.

Although complex models show an high degree of accuracy in reproducing epidemiological data, most of these models are too complex to be exploited for a model-based feedback design, especially for the early stages of the disease spread when few data are available. Moreover, dealing with simple epidemic models allows to identify the parameter values with small confidence intervals [5,36]. So, a trade-off between simplicity and accuracy is mandatory in the model formulation, especially when the model is used for building optimal control policies.

Several techniques have been proposed for NPIs planning, and in particular for the optimal open-loop and closed-loop design of lock-down phases. Most of them rely on multi-compartmental models of the epidemic spread, which are extended versions of the well-known SIR model; examples of these frameworks are SIDARTHE, exploited in [25] to design a Model Predictive Control (MPC) strategy to minimize the deaths for COVID-19, SIRQTHE in [11], where a multi-region scenario was adopted to design optimal control strategies during post-lockdown phases, SIRASD in [30], where an MPC approach is proposed to cope with COVID-19 contagion in Brazil, SIRCQTHE in [38], where a stochastic MPC problem is formulated to infer suitable restrictions on the mobility of different socioeconomic categories, and SIHRD in [29], exploited to guarantee safety against the spread of infectious diseases by viewing epidemiological models as control systems and by considering NPIs as control inputs. The drawback in adopting such comprehensive models is that they are difficult to identify, especially in the first epidemic spread, where urgent decisions have to be taken. This is the main motivation for our choice of a minimal SIRD model to describe COVID-19 transmission: it can be rapidly identified according to a short observation interval and, besides, we can benefit of the analytical solutions, that can be exploited when designing the optimization policy.

In a recently published paper [6], we proposed a technique to optimally design the lock-down in terms of starting and ending times, as well as of the number of isolated people. The proposed optimization approach aimed at containing the outbreak during the very first spreading period, on the basis of few and raw epidemiological data. In the present work, we extend the idea proposed in our previous paper, by addressing a trial-and-error procedure based on which the adopted restrictions are periodically revised every two weeks. The formulation of the optimization problem is based on a time-varying SIRD model which allows to reproduce the dynamic evolution of the disease with a minimal number of parameters and to take the continuously changing containment measures applied by the Italian government into account. Based on the underlying modeling assumptions, our optimal procedure is technically sound as long as relatively short intervention periods are addressed (i.e., from some months up to a few years). Indeed, for the sake of simplicity of the mathematical formulation, we intentionally disregard important epidemiological aspects arising over long time intervals, as the loss of immunity after healing, people reinfections, vaccinations, virus mutations etc.

Time-varying models are not a novelty in the COVID-19 modeling framework: we may cite, among the others, references focused on identification purposes, like [1,9], where the model parameters are given in terms of combinations of basis functions, and [7], where the identification is performed according to deep-learning algorithms; concerning the design of NPI control schemes, we mention [32], where linear state-dependent variations of the SIRD parameters are assumed and an optimal MPC problem minimizing both number of infections and confinement measures is proposed, and [17], where a SEIRD model with time-varying relative infection rate is used to design a control scheme that regulates the social distancing on the basis of five levels of lock-downs, seeking the minimization of the intensive care unit occupancy; recent SIRD-based MPC problems addressing the optimal planning of the social contact restrictions in Brasil are also proposed in [31,33], where the problem is formulated assuming a first order heuristic for the dynamical equation of the social distancing ratio. The main differences of our optimization problem compared to the control problems formulated in [17,31–33] are: (i) we directly minimize the total number of dead people at the end of a medium-term prediction interval (while in the mentioned works the reduction of deaths is an indirect consequence of the proposed objectives, basically looking for the infection reduction), (ii) we do not assume any specific value or explicit state-dependent relation for the contact rate, but its optimal level is directly inferred from the optimization output. We note that minimizing the total number of deaths is a less conservative approach than minimizing the current number of infections. However, as shown in the numerical results, the proposed optimal policy also reduces the maximal peak of infected individuals with respect to the real Italian case, thus resulting in a substantial reduced pressure on the local health structures. Moreover, the choice of making decisions on the present restriction policy based on the predicted cumulative deaths at the end of a forecast interval rather than on the current deaths is a cautious stance because of the observed delay between the adopted restrictions and the produced effects on the infection spread. We finally note that, although many interesting assumptions on the contact rate can be investigated, for the sake of generality we opt to leave its optimization free from specific modeling hypotheses.

The paper is organized as follows: Section 2 introduces the time-varying SIRD model and its parameter identification from COVID-19 Italian data. In Section 3, the optimization problem is formulated and an approximate real-time receding-horizon solution is proposed. Section 4 includes numerical simulations based on real data. Section 5 offers concluding remarks.

2. Model setting and identification from real data

2.1. Model

The formulation of the optimization problem is based on a classical mathematical representation of the epidemic dynamics. The model exploited is a SIRD ODE system which extends the SIR formulation by McKendrick and Kermack [26], by explicitly taking into account dead and healed among removed people. Since the period of interest is characterized by time-varying intervention measures adopted by the authorities to contain the disease outbreak, but also by an increasing preparedness of the health system in facing the emergency and the disease complications, we exploited a time-varying model formulation. For the sake of simplicity, we assume the model parameters to be piecewise-constant, changing every Δ days.

In particular, we denote by $\beta_k, \gamma_k, \nu_k \in \mathbb{R}_{>0}$ the relative infection rate, the per capita recovery and mortality rates, respectively, which are kept constant for any time $t \in [k\Delta, (k+1)\Delta)$ and switch at the beginning of each time interval $t = k\Delta$, $k = 0, 1, \ldots, K-1$, where the whole temporal period of interest is supposed to consist of K intervals.

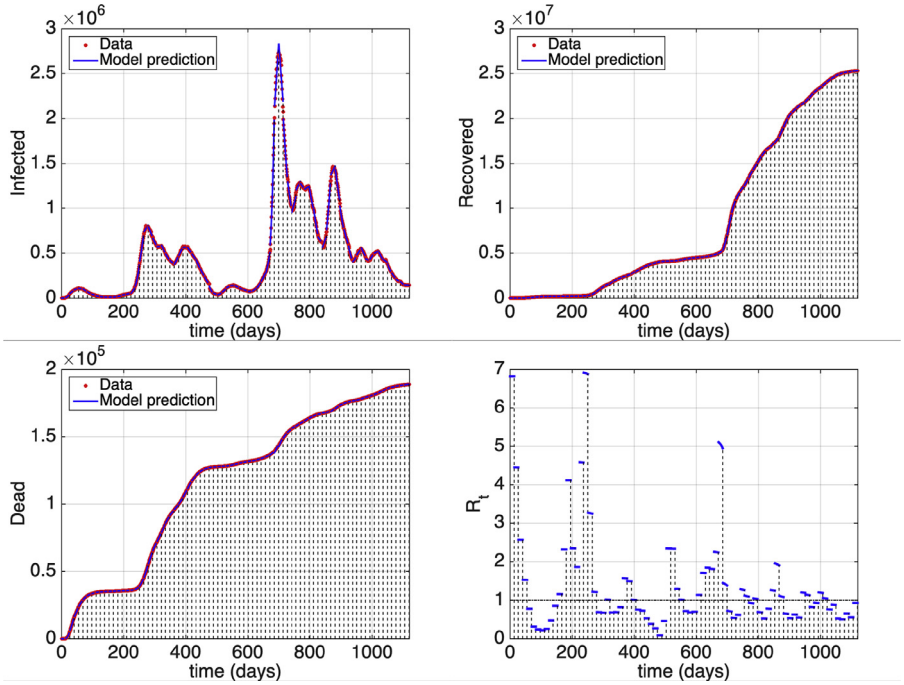

Fig. 1. Best fit on COVID-19 Italian data up to March 19, 2023. Panel A: daily number of infected. Panels B and C: total number of notified recovered and dead patients. Panel D: model-based prediction of the reproduction number. Red dots: ISS data [14]. Blue line: model prediction. (For interpretation of the references to color in this figure legend, the reader is referred to the web version of this article.)

On the basis of these assumptions, we define the following time-varying SIRD model:

$$\begin{cases} \dot{S}(t) = -\frac{\beta_k}{N} S(t) I(t), \\ \dot{I}(t) = \frac{\beta_k}{N}, S(t) I(t) - (\gamma_k + \nu_k) I(t), \\ \dot{R}(t) = \gamma_k I(t), \\ \dot{D}(t) = \nu_k I(t), \end{cases} \qquad t \in [k\Delta, (k+1)\Delta) \tag{1}$$

where the state variables $S(t)$, $I(t)$, $R(t)$, $D(t)$ represent the number of susceptibles, infectious, recovered and deceased, respectively, at time $t \in \mathbb{R}_{\geq 0}$ (expressed in days). Note that the total population size $S(t) + I(t) + R(t) + D(t) = N$ is constant for any time t according to the given formulation that is a realistic representation over a short time interval (which allows to neglect possible demographic changes).

Although the main features of the COVID-19 epidemics (like the presence of a relatively long period of incubation or the latency between infection and symptoms onset or the crucial role of the asymptomatic carriers on the infection spread) are now well known, we neglect such features opting for a "minimal" model representation (both in terms of compartment and parameter numbers) in order to simplify the formulation of the optimization problem. However, the time-varying structure adopted in the formulation above allows the SIRD model to efficiently describe the epidemiological data within short observation intervals, as it can be noticed from the fitting curves reported in Fig. 1.

Moreover, a further advantage of the adopted model structure is that its parameters are well identifiable in each observation interval on the basis of the few epidemiological data provided by the official sources, i.e. the number of (diagnosed) current infectious and the total number of dead and healed. Indeed, a significant drawback in adopting more accurate model representations is that they may face unidentifiability problems because of the insufficient information provided by the official data [5,6,36].

We finally make the following working assumptions:

- in the first interval ($k = 0$), no restrictions are applied yet or, at least, their effect can be reasonably neglected, provided that Δ is sufficiently short. This is regarded as *open-loop* condition;
- in the following periods ($k > 0$), governmental restrictions and personal containment measurements may only affect the infection rate β_k, while exogenous modifications only affect γ_k and ν_k. These include e.g. therapy improvements, seasonal changes, virus modifications.

Model (1) can be shortly restated in state-space form by defining the state vector $x(t) = [S(t) \quad I(t) \quad R(t) \quad D(t)]^T$ at all times $t \in [0, K\Delta]$. We denote by $\mathbf{x}(t, x_0, \beta, \gamma, \nu)$ as the forward solution of model (1) at time t assuming constant parameters (β, γ, ν) from time 0 (resulting in a time-invariant system). By a slight abuse of notation, we will let time $t \in [0, +\infty)$, thereby assuming $\mathbf{x}(t, x_0, \beta, \gamma, \nu)$ as the time evolution over a possibly infinite-horizon time length, when all three model parameters are supposed to be fixed.

We define $d_\Delta(x, \beta, \gamma, \nu)$ as the additional deaths, predicted at the end of a time interval Δ, with respect to those already present in state x (i.e. at the beginning of the same interval), computed as

$$d_\Delta(x, \beta, \gamma, \nu) = C \left(\mathbf{x}(\Delta, x, \beta, \gamma, \nu) - x \right), \tag{2}$$

where $C = [0 \quad 0 \quad 0 \quad 1]$ selects the last component of x. Intuitively, from (1), it readily comes that $d_\Delta(x, \beta, \gamma, \nu)$ is a monotonically increasing function of β when all the other quantities are fixed. Note that, given the initial condition x and the values of the parameters β, γ, and ν, closed-form expressions are available [6] to compute the values attained by the function $d_\Delta(x, \beta, \gamma, \nu)$.

2.2. Identification from COVID-19 Italian data

The identification of the SIRD parameters has been performed on the horizon $[0, K\Delta]$, based on the epidemiological data of the COVID-19 in Italy provided by the National Institute of Health of Italy (ISS). The data are published on the data repository GitHub

[14], edited by the national Civil Protection Department since February 24, 2020. The database collects a large amount of Italian data, as the cumulative number of cases, the number of currently infected people, hospitalized or not, the total number of healed and dead patients, the number of swab tests etc., daily updated and hierarchically organized at national, regional and provincial levels. For the purpose of SIRD identification we only exploit the national data on the number of current infected, total healed and dead people. At the moment of the manuscript editing, the data were updated up to March 19, 2023, covering approximately 3 years of COVID-19 pandemic.

Based on such data, the identification substantially reflects what happened in Italy according to an increasing awareness of the COVID-19 disease (parameters γ and ν) and to the Government restrictions and individual consciousness of social distancing (parameter β). The estimates of γ and ν will be exploited to build up a realistic scenario for the synthesis of the proposed optimal restriction policy aiming at modifying parameter β: the underlying working assumption is that parameters γ and ν do not depend on β, implying that recovery and healing from the COVID-19 disease do not depend on the relative infection rate.

Denoting by $\theta_k = (\beta_k, \gamma_k, \nu_k)$ the parameter vector of the kth interval $[k\Delta, (k+1)\Delta)$, and by $x(k\Delta) = (S(k\Delta)\ \ I(k\Delta)\ \ R(k\Delta)\ \ D(k\Delta))^T$ the related initial state vector, the identification procedure addressed the estimation of the family $\{(\bar{\theta}_k, \bar{x}(k\Delta)) \in \mathbb{R}^3_{>0} \times \mathbb{R}^4_{\geq 0}, k = 0, \ldots, K-1\}$, where $(\bar{\theta}_k, \bar{x}(k\Delta))$ denotes the best estimate of the pair $(\theta_k, x(k\Delta))$ for the kth interval. Note that, in order to make the parameter estimation of an interval independent of the previous estimates, the initial conditions of each interval have been identified in addition to the model parameters thus allowing to neglect the previous estimates of the parameters while identifying the ones of the kth interval.

The fitting procedure has been implemented in MATLAB environment, exploiting an Ordinary Least Squares (OLS) approach. The model parameters, with their 99% confidence intervals, have been estimated by means of the functions lscurvefit" and nlparci". The population size N has been fixed to 60317000, which is the value of Italian population on January 1st, 2020 [24].

The length Δ plays a crucial role in order to identify a trustworthy model. The smaller the value of Δ is, the better the data fitting is expected, at the cost of an increasing number of model parameters, with the drawback of possibly obtaining an underdetermined system and a consequent loss of accuracy in the parameter estimation (overfitting). To deal with such an issue, we decide to limit our investigation to four values of Δ, i.e. 1,2,3,4 weeks. The choice of Δ being multiple of 1 week is made to reduce the effect of random intraweek variations in data consequent to observed variations in the number of swab tests (typically occurring at weekends) [14]. The limit set to 4 weeks is oriented to make the model adaptive to possible mid-term modifications of the pandemic features. The identification interval Δ has been chosen according to a trade-off between the in-sample fitting error and the accuracy of the parameter estimation.

Concerning the model capability to faithfully reproduce the epidemiological data, we computed the Akaike Information Criterion (AIC) [2,3] for the aforementioned four different lengths of the observation interval Δ. The interested reader is referred to [27] for a deeper analysis about the Akaike Information Criterion. The analysis has been carried out according to different versions of AIC (normalized, raw, sample-size corrected criterion). All these versions reveal the same monotonic trend w.r.t. the size of the observation interval, showing an increasing prediction error when Δ increases. As an example, Table 1 reports the values of the normalized AIC (nAIC), computed for $\Delta = 7, 14, 21, 28$ days. The table shows that setting $\Delta = 7$ days is the best choice for maximizing the capability of the model to reproduce the available data.

Table 1
Normalized Akaike Information Criterion (nAIC) and Coefficient of Variation (CV) related to the ordinary least square data fitting (until March 19, 2023), performed for $\Delta = 7, 14, 21, 28$ days.

Δ	nAIC	CV (%)
7	34.18	9.275
14	37.85	4.254
21	40.14	2.681
28	42.23	2.758

Concerning the accuracy of the parameter estimation, we evaluated the Coefficient of Variation (CV) of the estimated parameters for the four candidate Δ values. Reasonably, the CV computation provides an approximately monotonic decreasing trend w.r.t. Δ up to the value of $\Delta = 21$ days, as shown by Table 1.

In summary, the opposite trends of the AIC and CV criteria prevent reaching a consensus clearly stating which one of the proposals is better to choose. In other words, the results in Table 1 show that $\Delta \in \{7, 14, 21\}$ days are all feasible choices (i.e. Pareto efficient solutions in the multi-objective optimization of model prediction error and parameter estimation accuracy), while $\Delta = 28$ days is not an optimal choice since it is strictly worse than $\Delta = 21$ days in both the targets (nAIC and CV). Our final choice is the intermediate one, namely $\Delta = 14$ days, since it produces a strong relative improvement (in terms of CV) with respect to $\Delta = 7$ days and better prediction results (in terms of nAIC) compared to $\Delta = 21$ days, which makes it the best trade-off between model prediction error and parameter estimation accuracy.

According to the whole period of data collection we set $K = 80$. Table A.1 in appendix reports the estimated values of the SIRD parameters for the 80 identification intervals obtained with $\Delta = 14$ days, while Fig. 1 shows the fitting curves compared with the official data. Panel D of Fig. 1 shows also the model-based evaluation of the effective reproduction number $(\bar{\beta}_k/(\bar{\gamma}_k + \bar{\nu}_k))S(t)/N$, $t \in [k\Delta, (k+1)\Delta)$, [23] for any estimation interval, which clearly highlights the two waves occurred in Italy since the COVID-19 appearance.

3. The optimization problem

In a recent research article [6], we formulated an optimization approach for planning lockdowns, which included the determination of the starting and conclusion times for lockdown measures, along with the optimal number of individuals to be isolated. In that paper, we achieved prevention of virus transmission by directly removing individuals from the susceptible sub-population.

In contrast, the following problem formulation focuses on simulating the progressive isolation of individuals due to government-imposed restrictions. These measures range from basic regulations that affect economic and social activities to more stringent measures that prohibit people from leaving their homes. This is modeled by reducing the contact rate to effectively limit virus transmission. In other words, we extend the idea proposed in our previous paper, by addressing a trial-and-error procedure based on which the adopted restrictions are periodically revised. The formulation of the optimization problem is based on the time-varying SIRD model introduced in the previous section, where the infectivity rate β_k is optimized in each interval of duration Δ, as we detail next.

Specifically, we assume a uniform mixing scenario within the population, denoted as N, and we incorporate the infection mechanism, which is characterized by the force of infection denoted as $\beta SI/N$, so that the constant parameter β_k related to the interval

$[k\Delta, (k+1)\Delta)$ can be expressed as [23]

$$\beta_k = c_k \chi, \tag{3}$$

where c_k is the per capita contact rate (i.e. the number of contacts that an individual has per time unit) during the same interval and χ is the contagion probability of an infected-susceptible contact, which is related to the virus aggressiveness and to the efficacy of the hosts' immune system. Note that, as already mentioned in the introduction, the mathematical framework is simplified and, for the control purposes, it disregards the effect of possibly important epidemiological aspects arising over long time intervals (e.g. virus mutations and massive vaccination). This results in the assumption of a contagion probability approximately constant over the whole observation period.

Therefore, denoting by β_0 the relative infectivity of the first Δ days, defined on the basis of the contact rate baseline c_0, $\beta_0 = c_0\chi$ (i.e. in the absence of social contact restrictions), the level of people isolation L_k^i in each time interval can be expressed by the relative reduction of social contacts w.r.t. the baseline, that is

$$L_k^i = \frac{c_0 - c_k}{c_0} = \frac{\beta_0 - \beta_k}{\beta_0}, \tag{4}$$

where (4) clearly belongs to $[0, 1]$ since β_k can be at most equal to β_0 (no restrictions) or at least zero (complete isolation). Since social contact restrictions heavily impact on people lives, not only for the obvious economic implications but also for psychological aspects, they unavoidably imply a cost J_E which grows when the size of isolated people increases (i.e. when c_k, β_k decrease). For instance, for each time interval such a cost can be evaluated by means of a quadratic term, properly penalizing larger deviations from the open-loop condition:

$$\left(\frac{\bar\beta_0 - \beta_k}{\bar\beta_0}\right)^2, \tag{5}$$

where $\bar\beta_0$ is the actual relative infectivity estimated for $k = 0$. Hence, the average (quadratic) economic cost over a finite time interval of duration $M\Delta$ can be modeled as:

$$J_E(\beta_k, \dots, \beta_{k+M-1}) = \frac{1}{M}\sum_{j=k}^{k+M-1}\left(\frac{\bar\beta_0 - \beta_j}{\bar\beta_0}\right)^2. \tag{6}$$

On the other hand, the epidemics implies a severe sanitary cost, primarily due to the number of people dying for the disease. In order to evaluate the sanitary impact of the interventions that we are going to adopt in each time interval, we predict at the beginning of kth interval $[k\Delta, (k+1)\Delta)$ the total number of deceased that a new policy (implemented from $k\Delta$ onward) will produce at the end of a finite time interval of duration $M\Delta$. Assuming to revise such a policy every Δ days, the cumulative number of deceased at the end of the prediction period will be given by the sum over the M intervals of the deceased (2) within each interval and will be obviously dependent on the sequence of the infectivities β_j, $j = k, \dots, k+M-1$. The number of deaths within each interval is minimal when $\beta_k = 0$ (complete isolation), since further infections are prevented and additional deaths can be produced only by the decreasing number of residual infected, while it reaches its maximal value when $\beta_k = \beta_0$. Therefore we can define the average (quadratic) health cost associated to the choice at $t = k\Delta$ as

$$J_H(x(k\Delta), \beta_k, \dots, \beta_{k+M-1}, \bar\gamma_{k-1}, \bar\nu_{k-1}) = \frac{1}{M}\sum_{j=k}^{k+M-1}\left(\frac{d_\Delta(x(j\Delta), \beta_j, \bar\gamma_{k-1}, \bar\nu_{k-1}) - d_\Delta(x(j\Delta), 0, \bar\gamma_{k-1}, \bar\nu_{k-1})}{d_\Delta(x(j\Delta), \bar\beta_0, \bar\gamma_{k-1}, \bar\nu_{k-1}) - d_\Delta(x(j\Delta), 0, \bar\gamma_{k-1}, \bar\nu_{k-1})}\right)^2, \tag{7}$$

where $x(j\Delta)$ is the state at the beginning of the jth interval $[j\Delta, (j+1)\Delta)$.

Note that $x(j\Delta)$ is completely known for $j = k$, since $t = k\Delta$ is the current time of evaluation, while it can be predicted for $j = k+1, \dots, k+M-1$ by integrating system (1) over the $(j-1)$th interval with the given value of β_{j-1}. Concerning the death and recovery rates, we keep at constant values the parameters γ_j, ν_j, $j = k, \dots, k+M-1$. Indeed, the estimates $\bar\gamma_{k-1}$, $\bar\nu_{k-1}$ (related to the $(k-1)$th interval) are exploited for the prediction of the long-term deaths (after M intervals) at $t = k\Delta$. This is a reasonable choice since at $t = k\Delta$ we do not know the death and recovery rates of the incoming intervals $[j\Delta, (j+1)\Delta)$, $j = k, \dots, k+M-1$ yet. So the best evaluation for γ_j, ν_j, $j = k, \dots, k+M-1$ is given by the estimation performed in the last time interval of data processing.

Real-time receding-horizon control

We formulate now a trial-and-error procedure aiming at optimizing the restrictions of social contacts and human activities. The procedure searches the best trade-off between health and economic costs, and it is revised periodically every Δ days. Hence, for the general kth interval, with $k = 1, 2, \dots$, we solve iteratively the following problem:

$$\begin{aligned}(\beta_k^*, \dots, \beta_{k+M-1}^*) = \arg \min_{\substack{\beta_k, \dots, \beta_{k+M-1} \in [0, \bar\beta_0] \\ \text{subject to (1),(2)}}} \big(&\alpha J_E(\beta_k, \dots, \beta_{k+M-1}) \\ &+ (1-\alpha) J_H(\tilde x(k\Delta), \beta_k, \dots, \beta_{k+M-1}, \bar\gamma_{k-1}, \bar\nu_{k-1})\big),\end{aligned} \tag{8}$$

where $\tilde x(k\Delta)$ is the actual state at the decision time $t = k\Delta$, affected by all the (possibly optimal) interventions actuated in the first $(k-1)$ control intervals.

Once the optimization problem (8) is solved, the first optimal infection rate β_k^* is implemented by means of government restrictions aimed at tuning the per capita contact rate c_k defined in Eq. (3). Such a rate can be tuned, e.g., by imposing restrictions on the mobility of the population also exploiting publicly available data, such as the Google mobility reports [22].

Note also that:

- at the decision time $t = k\Delta$ the sequence of infectivities β_j, $j = k, \dots, k+M-1$, is computed by solving a M-dimensional optimization problem (since the prediction of the health cost depends on the next M intervals); however only the first one $\beta_k^* = \beta_k$ is actually implemented along the interval $[k\Delta, (k+1)\Delta)$ as the intervention policy will be revised at $t = (k+1)\Delta$;
- there is no optimization in the first interval $k = 0$, i.e. $t \in [0, \Delta)$;
- the optimal value β_k^* evaluated at the beginning of the kth interval, i.e. at time $t = k\Delta$, depends on the number of deceased predicted at the end of the next $M\Delta$ intervals on the basis of the most recent estimation of recovery/mortality rates (i.e. the values $\bar\gamma_{k-1}$, $\bar\nu_{k-1}$) that are kept constant along the next M intervals; this is a basic feature of the well-known Model Predictive Control (MPC) method (see e.g. [10] for a survey on this topic);
- the state $\tilde x((k+1)\Delta)$ depends on the implementation of the suggested value β_k^* but also on the parameters $\bar\gamma_k$, $\bar\nu_k$ (which are unknown when β_k^* is computed, at $t = k\Delta$, but completely determined at the end of the kth optimization interval, at $t = (k+1)\Delta$);
- the coefficient $\alpha \in [0, 1]$ allows for differently weighing the normalized economic and health costs; in particular, the cost function in (8) provides the following limit situations for the extreme values of α:
  - for $\alpha = 0$, only the health cost matters ($J = J_H$) and then the complete isolation strategy $\beta_k^* = 0$ is optimal;
  - for $\alpha = 1$, only the economic cost matters ($J = J_E$) and then the open-loop strategy $\beta_k^* = \bar\beta_0$ leads to the optimality for any k.

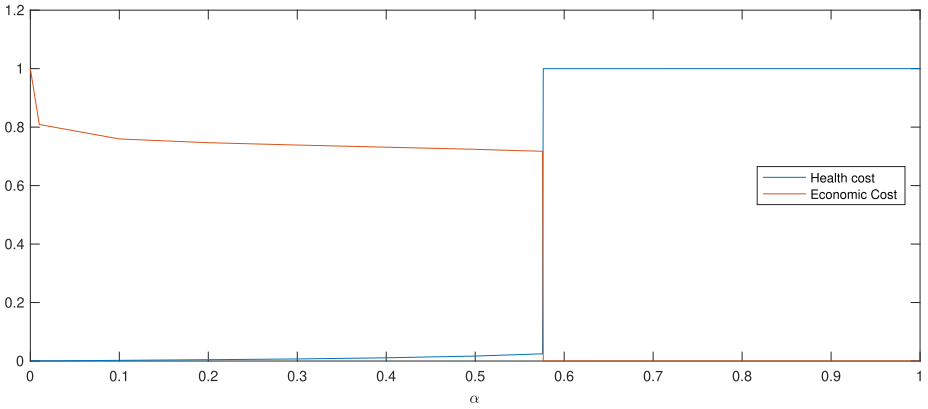

Fig. 2. Cumulative economic and health costs at the end of a long term time horizon ($\bar{K} = 52$) for $\alpha \in [0, 1]$.

We propose the following steps for the control procedure:

1. Interval 0 ("open-loop"), $[0, \Delta)$: identify the parameters $\bar{\beta}_0$, $\bar{\gamma}_0$, $\bar{\nu}_0$ from the first epidemiological data, until day Δ (do not perform any optimization);
2. Iterate the following steps for the interval $[k\Delta, (k+1)\Delta)$, with $k = 1, 2, \ldots, K-1$:
   (a) optimal planning: at the initial time $t = k\Delta$ evaluate the current state $\tilde{x}(k\Delta)$, determined by the policy actually implemented in interval $(k-1)$ (uncontrolled, for $k = 1$, or controlled, for $k > 1$), and compute the optimal solutions $(\beta_k^*, \beta_{k+1}^*, \ldots, \beta_{k+M-1}^*)$ of problem (8), assuming that the mortality and recovery rates are constant, over the entire prediction period $[k\Delta, (k+M)\Delta)$, and equal to $\bar{\gamma}_{k-1}$, $\bar{\nu}_{k-1}$ (estimated in interval $(k-1)$); note that the future states $x(j\Delta)$, $j = k+1, \ldots, k+M-1$, required for the computation of J_H, are predicted as $x(j\Delta) = \mathrm{x}(\Delta, x((j-1)\Delta), \beta_{j-1}, \bar{\gamma}_{k-1}, \bar{\nu}_{k-1})$, $j = k+1, \ldots, k+M-1$;
   (b) implementation and analysis: implement the optimal policy β_k^* during interval k and, at the end of the period, estimate from the epidemiological data the updated values of the recovery and mortality rates $\bar{\gamma}_k$, $\bar{\nu}_k$ that are required to solve problem (8) for interval $(k+1)$.

Since the weighting coefficient α deeply influences the result of the optimization problem (from complete isolation to open-loop condition) a suitable *a priori* tuning of its value is mandatory before implementing the proposed procedure. A way to reasonably tune α is to perform at the end of the first observation period (Δ days after the epidemic onset) a preliminary prediction evaluating the total health and economic costs possibly gathered at the end of a long-term period (for instance after a year). Such a tentative and raw evaluation can be performed exploiting the only knowledge acquired at $t = \Delta$, i.e. the estimated parameters $\bar{\beta}_0$, $\bar{\gamma}_0$, $\bar{\nu}_0$, identified from the epidemiological data of the first Δ days of the epidemic, as well as the current state $\tilde{x}(\Delta)$ (directly measured or estimated). In particular, denoting by $[0, \bar{K}\Delta)$ the long-term period of evaluation, the estimated death/recovery rates $\bar{\gamma}_0$, $\bar{\nu}_0$ are kept constant along the $\bar{K}$ intervals. In more detail, the evaluation of α can be performed by solving the following preliminary optimization problem:

$$\arg \min_{\substack{\beta \in [0, \bar{\beta}_0] \\ \text{subject to } (1),(2)}} \left(\alpha \left(\frac{\bar{\beta}_0 - \beta}{\bar{\beta}_0} \right)^2 + (1-\alpha) \left(\frac{d_{\bar{K}\Delta}(\tilde{x}(\Delta), \beta, \bar{\gamma}_0, \bar{\nu}_0) - d_{\bar{K}\Delta}(\tilde{x}(\Delta), 0, \bar{\gamma}_0, \bar{\nu}_0)}{d_{\bar{K}\Delta}(\tilde{x}(\Delta), \bar{\beta}_0, \bar{\gamma}_0, \bar{\nu}_0) - d_{\bar{K}\Delta}(\tilde{x}(\Delta), 0, \bar{\gamma}_0, \bar{\nu}_0)} \right)^2 \right), \tag{9}$$

where $d_{\bar{K}\Delta}$ denotes the additional deaths at the end of the prediction period $t = \bar{K}\Delta$.

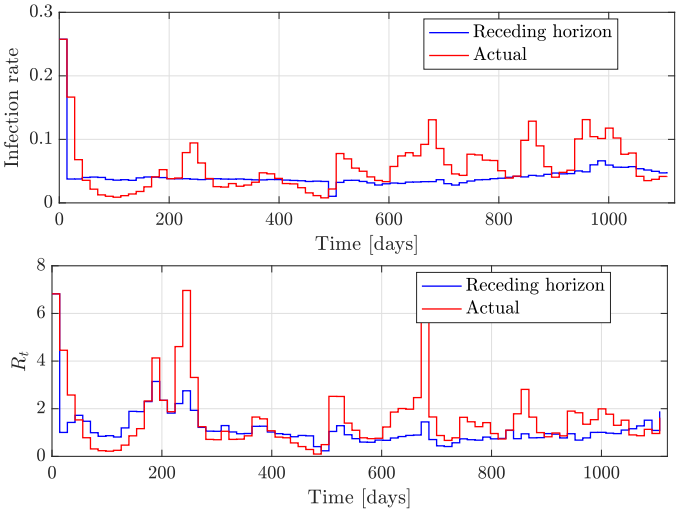

Fig. 3. Time behaviour of the optimal and real infectivities (top panel) and the related reproduction numbers (bottom panel) in $[0, K\Delta]$.

Eq. (9) approximately resembles (8) in the case of constant β_j, $j = 1, \ldots, M$ over the first M intervals after the open-loop one and with $M = \bar{K}$. Performing an evaluation of the economic cost component $\left(\frac{\bar{\beta}_0 - \beta}{\bar{\beta}_0} \right)^2$ and of the health cost component $\left(\frac{d_{\bar{K}\Delta}(\tilde{x}(\Delta), \beta, \bar{\gamma}_0, \bar{\nu}_0) - d_{\bar{K}\Delta}(\tilde{x}(\Delta), 0, \bar{\gamma}_0, \bar{\nu}_0)}{d_{\bar{K}\Delta}(\tilde{x}(\Delta), \bar{\beta}_0, \bar{\gamma}_0, \bar{\nu}_0) - d_{\bar{K}\Delta}(\tilde{x}(\Delta), 0, \bar{\gamma}_0, \bar{\nu}_0)} \right)^2$ by solving the simple optimization problem (9) for α ranging in (0,1), we obtain the cost behaviour as a function of α reported in Fig. 2. As expected from the problem formulation (9), the health cost increases (non-strictly) with α, since its weight in the cost function decreases linearly with α. As a matter of fact, the resulting behavior is almost discontinuous, with a trade-off between economic and health costs given by $\alpha \approx 0.575$. This allows to infer that there is a threshold of the health cost weight $(1-\alpha)$ (around $1 - 0.575 = 0.425$) below which the trade off is not meaningful and the trivial optimal solution is to impose no restrictions, i.e. $\beta = \bar{\beta}_0$ in (9), hence causing the maximum number of deaths. The solution $\beta = \bar{\beta}_0$ obtained for any $\alpha > 0.575$ implies, in particular, that the economic cost and the health cost are constantly equal to 0 and 1, respectively, so explaining the saturation of both the components of the cost for α large enough in Fig. 2.

As a consequence of the saturation behavior of the costs with respect to α, we consider in the following numerical section a value of $\alpha = 0.3$, resulting in $(1-\alpha) = 0.7$, such that human lives

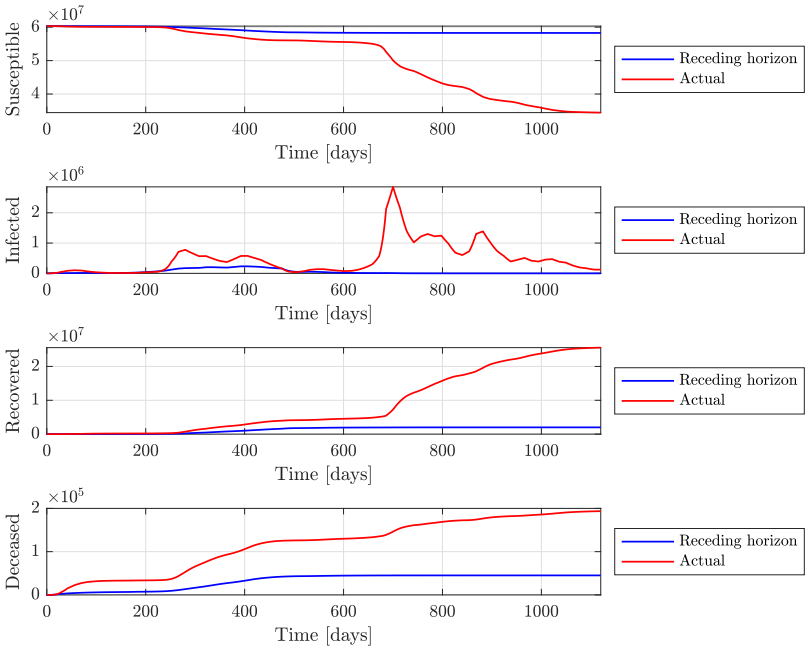

Fig. 4. Time behaviour of the state variables obtained by the integration of system (1) with the optimal infectivities β_k^*, $k = 0, 1, \ldots, K-1$.

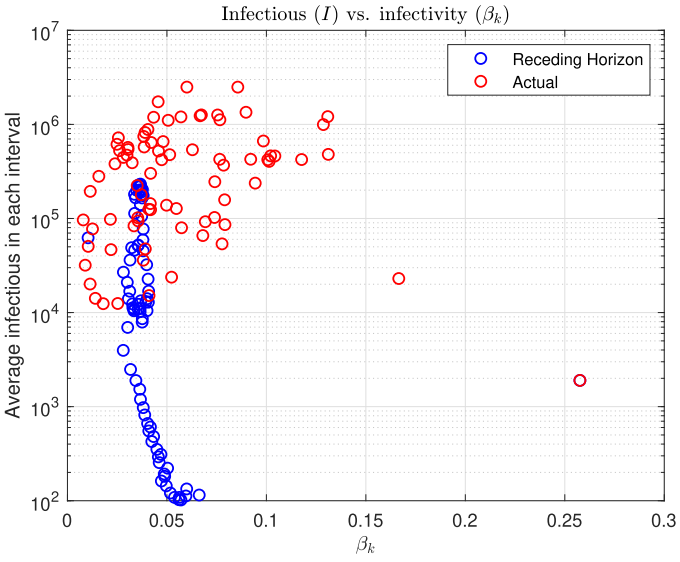

Fig. 5. Average infectious individuals (in semi-logarithmic scale) in each optimization interval $[k\Delta, (k+1)\Delta)$, $k = 0, \ldots, K$, versus infectivity β_k, $k = 0, \ldots, K$: comparison between optimal solution (blue circles) and solution fitted to the available data (red circles). (For interpretation of the references to colour in this figure legend, the reader is referred to the web version of this article.)

are sufficiently weighed to provide a non-trivial balance between health and economic cost, i.e. sparing a large amount of human lives, which was our original goal.

We note also that the choice of $\bar{K}$ is obviously arbitrary since we do not know when our emergency will end. However preliminary simulations showed that setting $\bar{K}\Delta > 1$ year basically provides the same results for any particular choice of $\bar{K}$ and Δ. We conservatively chose $\bar{K} = 52$, corresponding to a 2-year prediction period.

As the application of the optimal policy in each interval requires to solve the optimization problem (8) defined on a wider time range, i.e. $M\Delta$, we need to choose an adequate time horizon of prediction by suitably tuning M. Preliminary simulations showed that the choice $M = 6$ is a good compromise between the necessity to cope with the long-term policy effects, the model ability to make predictions, and the computational cost of determining a solution to the optimization problem (8).

4. Numerical simulations

In this section we show some results obtained solving the optimization problem (8) with $\alpha = 0.3$ and $M = 6$.

We recall that the solution of the optimization problem at the decision time $t = k\Delta$ depends on the current state $\tilde{x}(k\Delta)$, which in turn strongly depends on the containment measures actuated up to time $k\Delta$. Denoting by $\tilde{\beta}_{k-1}$ the real infection rate implemented in the $(k-1)$th interval, the current state at $t = k\Delta$ can be numerically evaluated as $\tilde{x}(k\Delta) = \mathbf{x}(\Delta, \tilde{x}((k-1)\Delta), \tilde{\beta}_{k-1}, \bar{\gamma}_{k-1}, \bar{\nu}_{k-1})$, as long as all the features of the $(k-1)$th interval are known (i.e. $\tilde{x}((k-1)\Delta)$, $\tilde{\beta}_{k-1}$, $\bar{\gamma}_{k-1}$, $\bar{\nu}_{k-1}$) and the SIRD model can be assumed to be a realistic representation of the real epidemic dynamics. Concerning the real infection rate $\tilde{\beta}_{k-1}$, we assume that:

- for $k = 1$, it coincides with the parameter identified from the non-controlled data of the "open-loop" interval, i.e. $\tilde{\beta}_0 = \bar{\beta}_0$;
- for $k > 1$, it is given by the optimal value computed for the controlled interval $k-1$ multiplied by an implementation error, i.e. $\tilde{\beta}_{k-1} = \beta_{k-1}^* \cdot \xi_{k-1}$, where the multiplicative noise ξ_{k-1} is uniformly distributed in the interval $[\underline{\xi}, \overline{\xi}]$ with constant upper and lower bounds $\underline{\xi}$ and $\overline{\xi}$.

Moreover, since we do not have available data resulting from the application of our policy to be exploited for the estimation of $\bar{\gamma}_{k-1}$, $\bar{\nu}_{k-1}$, we use the corresponding values identified in Section 2.2. Indeed, as we assumed that social contact restrictions do not influence these parameters (see Section 2.1), we can reasonably presume that they do not substantially change w.r.t. the ones identified from the data related to the real Italian policy. Finally, the value $\tilde{x}((k-1)\Delta)$ is trivially known since the optimization problem and the identification one have been already solved for the interval $[(j-2)\Delta, (j-1)\Delta)$.

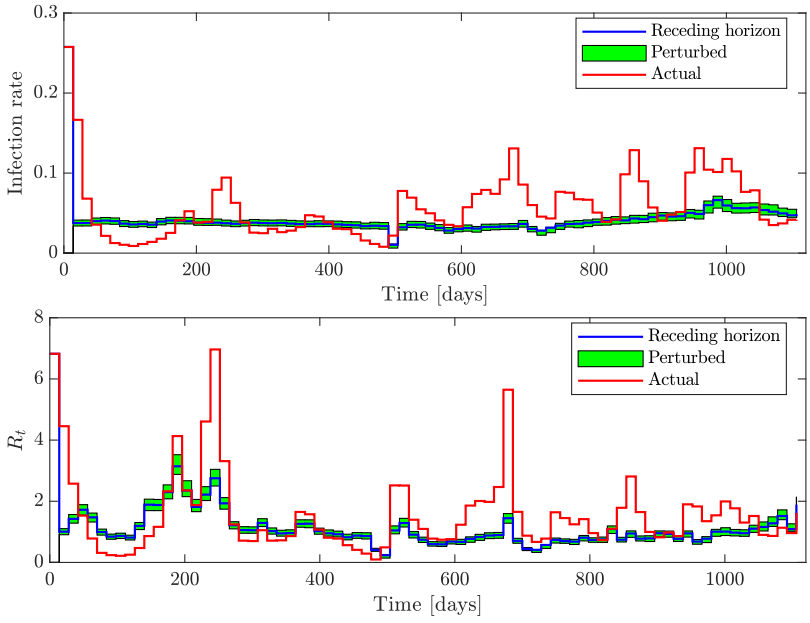

Fig. 6. Time behaviour of the optimal (receding-horizon), perturbed, and actual (estimated from the available data) infectivities (top panel) and reproduction numbers (bottom panel) in $[0, K\Delta]$, assuming for the perturbed infectivities a maximal implementation error in the contact rate equal to 10%. The envelope of the results obtained by means of 300 Monte Carlo perturbation simulations on the applied control law is also shown (in green). (For interpretation of the references to colour in this figure legend, the reader is referred to the web version of this article.)

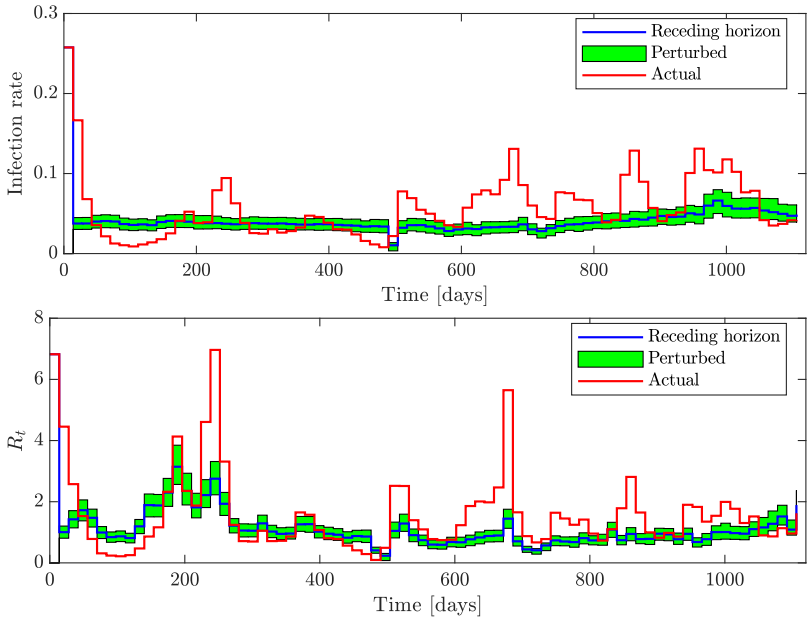

Fig. 7. Time behaviour of the optimal (receding-horizon), perturbed, and actual (estimated from the available data) infectivities (top panel) and reproduction numbers (bottom panel) in $[0, K\Delta]$, assuming for the perturbed infectivities a maximal implementation error in the contact rate equal to 20%. The envelope of the results obtained by means of 300 Monte Carlo perturbation simulations on the applied control law is also shown (in green). (For interpretation of the references to colour in this figure legend, the reader is referred to the web version of this article.)

Let us assume first to actuate perfectly the optimal restrictions suggested by the receding-horizon algorithm, without committing any implementation errors, that is $\xi_{k-1} = 1$ and then $\tilde{\beta}_{k-1} = \beta^*_{k-1}$, $k > 1$.

Figs. 3–4 show the comparisons between the optimal policy and the real containment measures adopted by the Italian government. In particular, Fig. 3 compares the optimal infectivities β^*_k, $k = 1, \ldots, (K-1)\Delta$, with respect to the estimation $\tilde{\beta}_k$, $k = 1, \ldots, (K-1)\Delta$, inferred from the Italian epidemiological data [14]. The figure shows how the optimal policy suggests to suddenly reduce the human contacts, as soon as the first observation interval ends. After the first strong revision of β^*_1, the policy suggests to smoothly change β^*_k during the entire control period. Conversely, the real containment measures produced an abrupt variation of $\tilde{\beta}_k$.

Accordingly, the comparison between the optimal value of the reproduction number $R^*_k = \left(\dfrac{\beta^*_k}{\bar{\gamma}_k + \bar{\nu}_k}\dfrac{\tilde{S}(k\Delta)}{N}\right)$ and the observed one $\tilde{R}_k = \left(\dfrac{\tilde{\beta}_k}{\bar{\gamma}_k + \bar{\nu}_k}\dfrac{\tilde{S}(k\Delta)}{N}\right)$, where $\tilde{S}(k\Delta)$ provides the number of susceptibles at $t = k\Delta$ corresponding to the policy (optimal, β^*_{k-1}, or observed, $\tilde{\beta}_{k-1}$) actually implemented in interval $(k-1)$, shows a

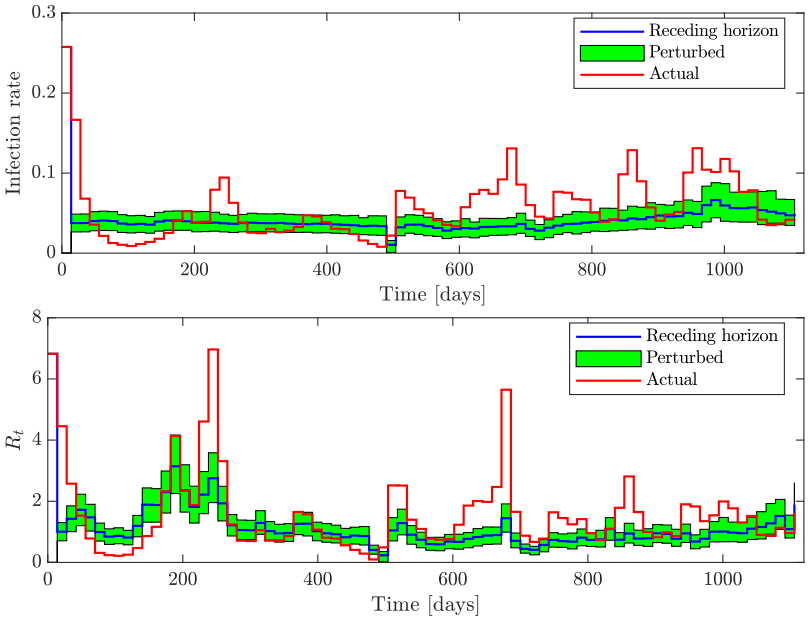

Fig. 8. Time behaviour of the optimal (receding-horizon), perturbed, and actual (estimated from the available data) infectivities (top panel) and reproduction numbers (bottom panel) in $[0, K\Delta]$, assuming for the perturbed infectivities a maximal implementation error in the contact rate equal to 30%. The envelope of the results obtained by means of 300 Monte Carlo perturbation simulations on the applied control law is also shown (in green). (For interpretation of the references to colour in this figure legend, the reader is referred to the web version of this article.)

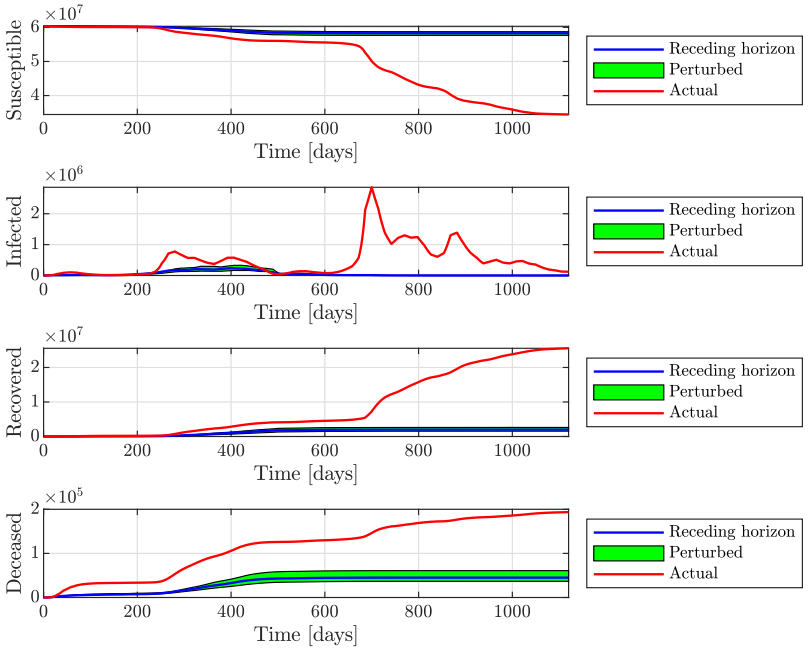

Fig. 9. Time behaviour of the state variables obtained by the integration of system (1) with the perturbed infectivities $\tilde{\beta}_k$, $k = 0, 1, \ldots, K-1$, letting the maximal implementation error be equal to 10%. The envelope of the results obtained by means of 300 Monte Carlo perturbation simulations on the applied control law is also shown (in green). (For interpretation of the references to colour in this figure legend, the reader is referred to the web version of this article.)

more uniform time-behaviour of the optimal policy that progressively drives the reproduction number in a neighbourhood of one, containing its oscillations, thus managing to mitigate the effects of the second wave, as it clearly appears in Fig. 3.

The main gain of the optimal policy is shown by Fig. 4 where the strong reduction of deaths can be inferred by the comparisons between the cumulative deaths (at $t = K\Delta$) produced by the optimal policy and the real one. Indeed, the optimal policy allows to reduce the total number of deaths by 76.71% with respect to the real containment actions. Such a strong saving of human lives is also associated to a light reduction of the economic costs (computed by Eq. (6) with $M = K$) by about 1% compared to the real interventions.

We finally note that the proposed MPC approach strictly controls the relative infectivity within a narrow variation interval and produces a substantial reduction of the mean infected during each control interval w.r.t. the observed case (see Fig. 5). Moreover, as shown by Fig. 4, the maximal number of current infected people is substantially lower than the real peaks reached by the two main epidemic waves occurred in Italy. Indeed, the maximum of infected

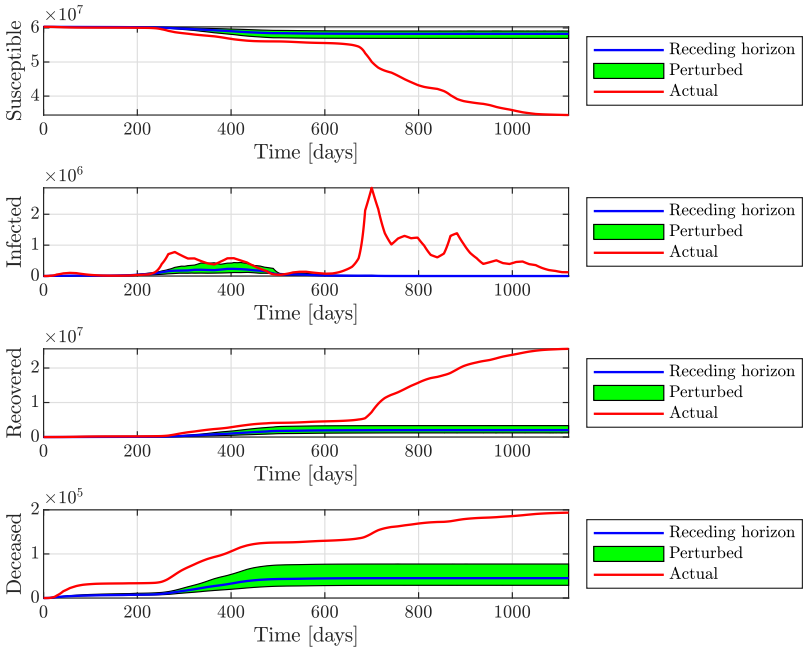

Fig. 10. Time behaviour of the state variables obtained by the integration of system (1) with the perturbed infectivities $\tilde{\beta}_k$, $k = 0, 1, \ldots, K-1$, letting the maximal implementation error be equal to 20%. The envelope of the results obtained by means of 300 Monte Carlo perturbation simulations on the applied control law is also shown (in green). (For interpretation of the references to colour in this figure legend, the reader is referred to the web version of this article.)

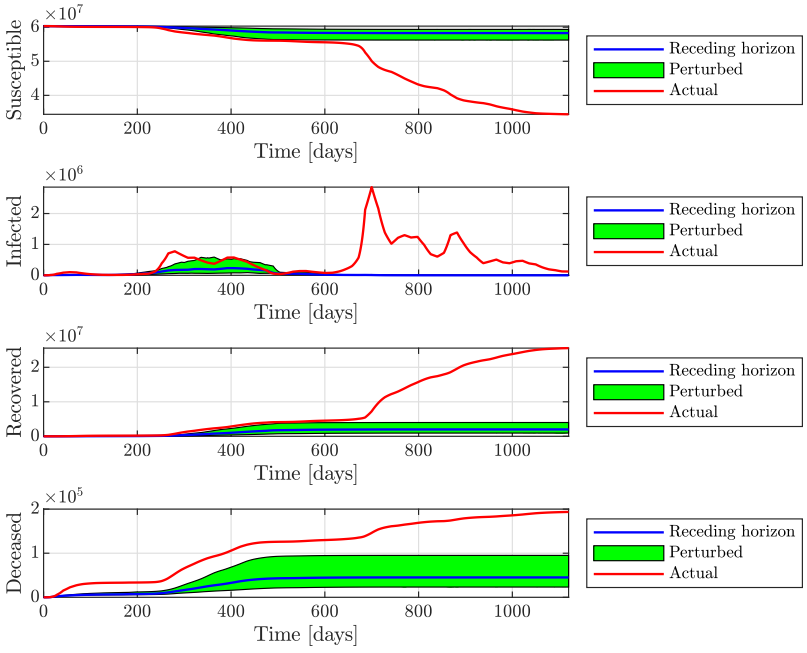

Fig. 11. Time behaviour of the state variables obtained by the integration of system (1) with the perturbed infectivities $\tilde{\beta}_k$, $k = 0, 1, \ldots, K-1$, letting the maximal implementation error be equal to 30%. The envelope of the results obtained by means of 300 Monte Carlo perturbation simulations on the applied control law is also shown (in green). (For interpretation of the references to colour in this figure legend, the reader is referred to the web version of this article.)

reached in the optimal case is 232 thousand individuals, against 2.855 millions individuals obtained using the real policy, which implies a definitely lower pressure on the hospitals and a higher capacity of the local health structures in sustaining patients.

Let us assume now to commit an error in implementing the optimal restrictions. Monte Carlo simulations have been carried out to evaluate the performance of the proposed control strategies by either letting $[\underline{\xi}, \overline{\xi}] = [0.9, 1.1]$, $[\underline{\xi}, \overline{\xi}] = [0.8, 1.2]$, or $[\underline{\xi}, \overline{\xi}] = [0.7, 1.3]$, i.e. by considering implementation errors of the desired policy up to 10%, 20%, or 30%, respectively. Figs. 6–8 show the comparisons, in terms of infectivities and reproduction numbers, between the theoretical optimal policy (without implementation error), the real containment measures adopted by the Italian government, and the optimal policy actually implemented (obtained by randomly perturbing the optimal one within relative bounds $[\underline{\xi}, \overline{\xi}]$), for a maximal implementation error equal to 10%, 20%, or 30%, respectively. Figs. 9–11 present analogous comparisons for the time course of the state variables, along with the envelope of the results obtained by means of 300 Monte Carlo perturbation simulations on the applied control law.

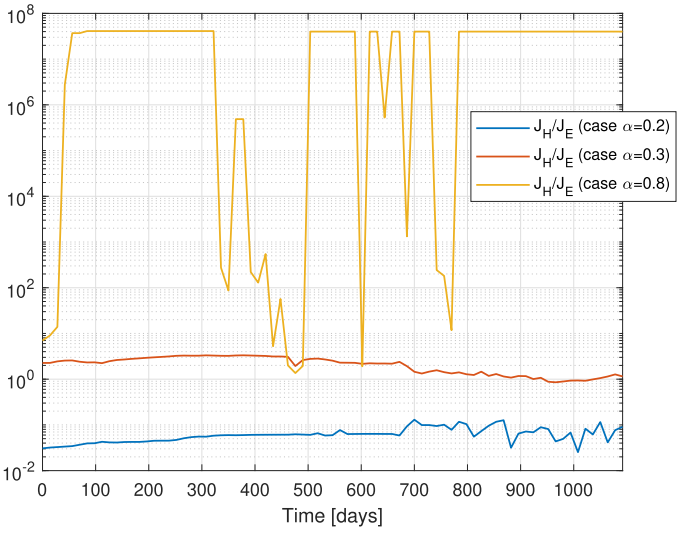

Fig. 12. Time behaviour (in semi-logarithmic scale) of the ratio J_H/J_E for the choices of $\alpha = 0.2$ (blue line), $\alpha = 0.3$ (red line), $\alpha = 0.8$ (yellow line). (For interpretation of the references to colour in this figure legend, the reader is referred to the web version of this article.)

As shown by such figures, the proposed method is robust with respect to variations in the actually implemented control. In fact, even in the case that the control policy is implemented with the largest error scenario (up to 30%), the outcome of the receding-horizon control is similar to the ideal one (reported in Fig. 3) obtained without accounting for the implementation error, producing at $t = K\Delta$ a reduction of the total number of deaths by at least 50.93% w.r.t. the real case.

We finally note that the value $\alpha = 0.3$ (used for all the above numerical results), chosen on the basis of the *a priori* exploration of Fig. 2, actually provides a fair trade-off between the two terms of the cost function. The *a posteriori* analysis reported in Fig. 12 shows the time behaviour of the ratio J_H/J_E obtained by solving problem (8) with $\alpha = 0.3$, with a lower value, i.e. $\alpha = 0.2$, and with a higher value (beyond the threshold 0.575), i.e. $\alpha = 0.8$. The figure shows that for $\alpha = 0.3$ the two costs are quite balanced, while moving away from this trade-off value one cost can exceed the other one by some orders of magnitude. Indeed, we have a mean ratio $< J_H/J_E >= 2.16$ for $\alpha = 0.3$, while the ratio substantially reduces to $< J_H/J_E >= 6.36 \cdot 10^{-2}$ for $\alpha = 0.2$ and strongly increases to $< J_H/J_E >= 2.91 \cdot 10^7$ for $\alpha = 0.8$.

5. Discussion

A framework based on a time-varying SIRD model has been proposed for the real-time optimization of non-pharmaceutical interventions during epidemics. Despite its simplicity, such a class of models has been demonstrated capable of capturing the essential features of an epidemic disease. In fact, allowing for parametric variations, these models can accurately adapt to real data.

An optimization problem over a receding horizon has been formulated to determine the optimal sequence of infection rates that balances health and economic costs. Such infection rates have been assumed to be actuated via government containment measures. The effectiveness of such an approach has been validated via numerical simulations based on the real data of the Italian COVID-19 emergency. The results of such simulations highlighted the potential of the proposed approach that may allow to decrease both the economic and health costs by suitably designing the "ideal" infectivity rate to be guaranteed in each time interval and consequently planning the corresponding restrictions of the human contacts. The simulations highlight that the "ideal" implementation of the optimal policy (i.e. without errors compared with the theoretical computation) is able to reduce the total number of deaths by 76.71% with respect to the real case, producing also a mild reduction of the economic cost. As a further advantage, the proposed technique with "ideal" implementation substantially reduces also the maximal number of concomitant infected individuals, producing a 91.88% of decrease with respect to the real case, thus resulting in a reduced pressure on the local health structures. Moreover, the results show that even in the worst-case scenario in which the optimal policy is implemented with an error up to 30% with respect to the theoretical computation, a significant reduction of deaths by about 50.93% compared to the real case is obtained, confirming the robustness of the proposed approach.

Declaration of Competing Interest

The authors declare that they have no known competing financial interests or personal relationships that could have appeared to influence the work reported in this paper.

Appendix A. Tables of estimates and confidence intervals for the SIRD model parameters

Table A.1
Estimates and 99% confidence intervals of the SIRD parameters for the 80 considered intervals of $\Delta = 14$ days.

Interval	β_k	γ_k	ν_k	CI_{β_k}	CI_{γ_k}	CI_{ν_k}
1	2.58e-01	2.59e-02	1.18e-02	[2.47e-01, 2.69e-01]	[2.04e-02, 3.14e-02]	[6.41e-03, 1.73e-02]
2	1.67e-01	2.09e-02	1.65e-02	[1.60e-01, 1.73e-01]	[1.76e-02, 2.42e-02]	[1.32e-02, 1.98e-02]
3	6.81e-02	1.57e-02	1.07e-02	[6.33e-02, 7.28e-02]	[1.30e-02, 1.84e-02]	[8.00e-03, 1.34e-02]
4	3.55e-02	1.78e-02	5.45e-03	[3.41e-02, 3.70e-02]	[1.69e-02, 1.86e-02]	[4.60e-03, 6.30e-03]
5	2.16e-02	2.42e-02	3.44e-03	[2.00e-02, 2.31e-02]	[2.33e-02, 2.51e-02]	[2.54e-03, 4.33e-03]
6	1.26e-02	3.78e-02	2.57e-03	[9.24e-03, 1.60e-02]	[3.58e-02, 3.97e-02]	[6.42e-04, 4.51e-03]
7	1.04e-02	4.19e-02	1.89e-03	[6.57e-03, 1.43e-02]	[3.97e-02, 4.42e-02]	[−3.33e-04, 4.12e-03]
8	8.93e-03	3.93e-02	2.00e-03	[4.77e-03, 1.31e-02]	[3.68e-02, 4.17e-02]	[−4.01e-04, 4.40e-03]
9	1.14e-02	4.36e-02	1.33e-03	[8.25e-03, 1.45e-02]	[4.18e-02, 4.55e-02]	[−4.75e-04, 3.14e-03]
10	1.40e-02	2.86e-02	1.12e-03	[1.09e-02, 1.71e-02]	[2.68e-02, 3.04e-02]	[−6.69e-04, 2.91e-03]
11	1.80e-02	2.00e-02	8.66e-04	[1.53e-02, 2.06e-02]	[1.85e-02, 2.15e-02]	[−6.56e-04, 2.39e-03]
12	2.53e-02	2.12e-02	5.76e-04	[2.25e-02, 2.80e-02]	[1.96e-02, 2.27e-02]	[−1.01e-03, 2.17e-03]
13	4.10e-02	1.63e-02	1.35e-03	[3.70e-02, 4.50e-02]	[1.40e-02, 1.86e-02]	[−9.35e-04, 3.63e-03]
14	5.23e-02	1.24e-02	2.87e-04	[5.04e-02, 5.43e-02]	[1.13e-02, 1.35e-02]	[−8.19e-04, 1.39e-03]
15	3.81e-02	1.59e-02	2.90e-04	[3.70e-02, 3.92e-02]	[1.53e-02, 1.65e-02]	[−3.46e-04, 9.27e-04]

(*continued on next page*)

Table A.1 (*continued*)

Interval	β_k	γ_k	ν_k	CI_{β_k}	CI_{γ_k}	CI_{ν_k}
16	3.91e-02	2.05e-02	4.04e-04	[3.75e-02, 4.08e-02]	[1.95e-02, 2.14e-02]	[−5.44e-04, 1.35e-03]
17	7.92e-02	1.67e-02	4.88e-04	[7.53e-02, 8.30e-02]	[1.45e-02, 1.89e-02]	[−1.69e-03, 2.67e-03]
18	9.44e-02	1.28e-02	7.28e-04	[9.31e-02, 9.57e-02]	[1.21e-02, 1.36e-02]	[−8.13e-06, 1.46e-03]
19	6.28e-02	1.81e-02	8.72e-04	[5.96e-02, 6.61e-02]	[1.63e-02, 1.99e-02]	[−9.52e-04, 2.70e-03]
20	3.84e-02	2.99e-02	9.22e-04	[3.49e-02, 4.19e-02]	[2.79e-02, 3.19e-02]	[−1.04e-03, 2.88e-03]
21	2.56e-02	3.50e-02	9.28e-04	[2.32e-02, 2.80e-02]	[3.37e-02, 3.64e-02]	[−3.94e-04, 2.25e-03]
22	2.49e-02	3.48e-02	8.53e-04	[2.26e-02, 2.72e-02]	[3.35e-02, 3.61e-02]	[−4.05e-04, 2.11e-03]
23	3.04e-02	2.81e-02	8.39e-04	[2.92e-02, 3.17e-02]	[2.74e-02, 2.88e-02]	[1.40e-04, 1.54e-03]
24	2.62e-02	3.59e-02	8.93e-04	[2.39e-02, 2.85e-02]	[3.46e-02, 3.72e-02]	[−3.77e-04, 2.16e-03]
25	2.81e-02	3.80e-02	9.09e-04	[2.67e-02, 2.95e-02]	[3.72e-02, 3.88e-02]	[1.37e-04, 1.68e-03]
26	3.25e-02	3.70e-02	7.91e-04	[3.08e-02, 3.43e-02]	[3.60e-02, 3.80e-02]	[−1.64e-04, 1.75e-03]
27	4.74e-02	2.80e-02	6.83e-04	[4.59e-02, 4.88e-02]	[2.72e-02, 2.88e-02]	[−1.21e-04, 1.49e-03]
28	4.58e-02	2.83e-02	7.20e-04	[4.43e-02, 4.72e-02]	[2.75e-02, 2.92e-02]	[−7.96e-05, 1.52e-03]
29	3.86e-02	3.51e-02	7.75e-04	[3.74e-02, 3.97e-02]	[3.45e-02, 3.58e-02]	[1.69e-04, 1.38e-03]
30	3.04e-02	3.69e-02	8.23e-04	[2.91e-02, 3.18e-02]	[3.61e-02, 3.76e-02]	[8.44e-05, 1.56e-03]
31	2.99e-02	3.77e-02	6.73e-04	[2.86e-02, 3.13e-02]	[3.69e-02, 3.84e-02]	[−4.99e-05, 1.40e-03]
32	2.39e-02	4.18e-02	5.64e-04	[2.24e-02, 2.54e-02]	[4.10e-02, 4.26e-02]	[−2.51e-04, 1.38e-03]
33	1.58e-02	3.79e-02	4.91e-04	[1.43e-02, 1.72e-02]	[3.71e-02, 3.87e-02]	[−2.99e-04, 1.28e-03]
34	1.15e-02	3.94e-02	3.63e-04	[7.89e-03, 1.50e-02]	[3.74e-02, 4.13e-02]	[−1.56e-03, 2.28e-03]
35	7.94e-03	8.22e-02	3.65e-04	[−1.67e-02, 3.26e-02]	[6.82e-02, 9.62e-02]	[−1.29e-02, 1.37e-02]
36	2.19e-02	4.40e-02	4.61e-04	[1.75e-02, 2.63e-02]	[4.16e-02, 4.64e-02]	[−1.91e-03, 2.83e-03]
37	7.77e-02	3.06e-02	2.40e-04	[7.08e-02, 8.46e-02]	[2.69e-02, 3.43e-02]	[−3.42e-03, 3.90e-03]
38	6.93e-02	2.73e-02	2.15e-04	[6.59e-02, 7.27e-02]	[2.55e-02, 2.92e-02]	[−1.60e-03, 2.03e-03]
39	5.47e-02	3.89e-02	3.23e-04	[5.22e-02, 5.73e-02]	[3.75e-02, 4.03e-02]	[−1.03e-03, 1.68e-03]
40	4.98e-02	4.51e-02	4.05e-04	[4.73e-02, 5.23e-02]	[4.37e-02, 4.64e-02]	[−9.34e-04, 1.74e-03]
41	4.09e-02	5.21e-02	4.63e-04	[3.84e-02, 4.34e-02]	[5.07e-02, 5.34e-02]	[−8.64e-04, 1.79e-03]
42	3.53e-02	4.70e-02	5.22e-04	[3.29e-02, 3.78e-02]	[4.57e-02, 4.84e-02]	[−7.86e-04, 1.83e-03]
43	3.35e-02	4.36e-02	4.41e-04	[3.16e-02, 3.53e-02]	[4.26e-02, 4.46e-02]	[−5.40e-04, 1.42e-03]
44	5.73e-02	4.60e-02	5.10e-04	[5.34e-02, 6.13e-02]	[4.39e-02, 4.82e-02]	[−1.59e-03, 2.61e-03]
45	7.39e-02	3.93e-02	5.12e-04	[7.15e-02, 7.63e-02]	[3.80e-02, 4.05e-02]	[−7.47e-04, 1.77e-03]
46	7.90e-02	3.89e-02	4.37e-04	[7.72e-02, 8.08e-02]	[3.79e-02, 3.99e-02]	[−5.19e-04, 1.39e-03]
47	7.41e-02	3.71e-02	3.56e-04	[7.23e-02, 7.58e-02]	[3.61e-02, 3.80e-02]	[−5.69e-04, 1.28e-03]
48	9.21e-02	3.70e-02	3.37e-04	[8.72e-02, 9.70e-02]	[3.45e-02, 3.96e-02]	[−2.19e-03, 2.86e-03]
49	1.31e-01	2.30e-02	2.12e-04	[1.25e-01, 1.37e-01]	[1.98e-02, 2.61e-02]	[−2.91e-03, 3.33e-03]
50	8.56e-02	5.16e-02	2.10e-04	[8.04e-02, 9.08e-02]	[4.90e-02, 5.42e-02]	[−2.32e-03, 2.74e-03]
51	6.00e-02	6.84e-02	2.20e-04	[5.28e-02, 6.73e-02]	[6.48e-02, 7.20e-02]	[−3.22e-03, 3.66e-03]
52	4.56e-02	6.79e-02	1.79e-04	[4.32e-02, 4.79e-02]	[6.68e-02, 6.90e-02]	[−9.10e-04, 1.27e-03]
53	4.33e-02	5.54e-02	1.70e-04	[3.86e-02, 4.81e-02]	[5.32e-02, 5.76e-02]	[−1.99e-03, 2.33e-03]
54	7.66e-02	4.66e-02	9.53e-05	[6.97e-02, 8.36e-02]	[4.35e-02, 4.98e-02]	[−3.01e-03, 3.20e-03]
55	7.55e-02	5.19e-02	1.25e-04	[7.28e-02, 7.81e-02]	[5.07e-02, 5.31e-02]	[−1.04e-03, 1.28e-03]
56	6.73e-02	5.39e-02	1.03e-04	[6.47e-02, 6.99e-02]	[5.28e-02, 5.51e-02]	[−1.02e-03, 1.22e-03]
57	6.67e-02	4.70e-02	1.20e-04	[6.33e-02, 7.01e-02]	[4.55e-02, 4.85e-02]	[−1.32e-03, 1.56e-03]
58	5.06e-02	5.27e-02	1.08e-04	[4.74e-02, 5.39e-02]	[5.14e-02, 5.41e-02]	[−1.25e-03, 1.47e-03]
59	3.90e-02	5.34e-02	1.11e-04	[3.47e-02, 4.34e-02]	[5.15e-02, 5.52e-02]	[−1.68e-03, 1.90e-03]
60	4.21e-02	3.82e-02	8.73e-05	[3.87e-02, 4.55e-02]	[3.68e-02, 3.96e-02]	[−1.30e-03, 1.47e-03]
61	9.85e-02	5.51e-02	3.77e-05	[8.55e-02, 1.11e-01]	[4.97e-02, 6.04e-02]	[−5.18e-03, 5.26e-03]
62	1.29e-01	4.57e-02	9.89e-05	[1.24e-01, 1.33e-01]	[4.38e-02, 4.75e-02]	[−1.70e-03, 1.90e-03]
63	8.97e-02	5.44e-02	1.30e-04	[8.43e-02, 9.52e-02]	[5.22e-02, 5.65e-02]	[−1.95e-03, 2.21e-03]
64	5.70e-02	5.71e-02	1.34e-04	[5.39e-02, 6.02e-02]	[5.59e-02, 5.83e-02]	[−1.04e-03, 1.31e-03]
65	4.04e-02	4.91e-02	1.16e-04	[3.37e-02, 4.72e-02]	[4.65e-02, 5.17e-02]	[−2.40e-03, 2.63e-03]
66	4.81e-02	4.89e-02	1.14e-04	[4.44e-02, 5.17e-02]	[4.75e-02, 5.03e-02]	[−1.23e-03, 1.46e-03]
67	5.14e-02	5.96e-02	1.02e-04	[4.32e-02, 5.96e-02]	[5.65e-02, 6.27e-02]	[−2.89e-03, 3.09e-03]
68	1.01e-01	5.29e-02	8.95e-05	[9.08e-02, 1.11e-01]	[4.93e-02, 5.66e-02]	[−3.46e-03, 3.64e-03]
69	1.31e-01	7.15e-02	1.19e-04	[1.24e-01, 1.38e-01]	[6.90e-02, 7.41e-02]	[−2.30e-03, 2.54e-03]
70	1.04e-01	7.71e-02	1.68e-04	[9.97e-02, 1.09e-01]	[7.55e-02, 7.88e-02]	[−1.44e-03, 1.78e-03]
71	1.01e-01	6.57e-02	1.69e-04	[9.48e-02, 1.08e-01]	[6.33e-02, 6.80e-02]	[−2.11e-03, 2.45e-03]
72	1.18e-01	5.89e-02	1.83e-04	[1.14e-01, 1.22e-01]	[5.74e-02, 6.03e-02]	[−1.19e-03, 1.55e-03]
73	1.02e-01	5.75e-02	1.98e-04	[9.78e-02, 1.06e-01]	[5.60e-02, 5.90e-02]	[−1.26e-03, 1.66e-03]
74	7.65e-02	5.85e-02	2.46e-04	[7.23e-02, 8.08e-02]	[5.70e-02, 5.99e-02]	[−1.18e-03, 1.68e-03]
75	7.85e-02	5.14e-02	2.67e-04	[7.05e-02, 8.65e-02]	[4.87e-02, 5.42e-02]	[−2.41e-03, 2.94e-03]
76	4.18e-02	4.62e-02	2.21e-04	[3.77e-02, 4.59e-02]	[4.48e-02, 4.76e-02]	[−1.14e-03, 1.59e-03]
77	3.51e-02	4.02e-02	2.37e-04	[2.87e-02, 4.14e-02]	[3.81e-02, 4.24e-02]	[−1.89e-03, 2.37e-03]
78	3.71e-02	3.25e-02	2.13e-04	[2.98e-02, 4.45e-02]	[3.01e-02, 3.50e-02]	[−2.23e-03, 2.66e-03]
79	4.17e-02	4.32e-02	2.12e-04	[3.18e-02, 5.15e-02]	[3.98e-02, 4.65e-02]	[−3.07e-03, 3.50e-03]
80	4.18e-02	2.55e-02	2.06e-04	[3.97e-02, 4.38e-02]	[2.49e-02, 2.62e-02]	[−4.74e-04, 8.86e-04]

References

[1] R. Abolpour, S. Siamak, M. Mohammadi, P. Moradi, M. Dehghani, Linear parameter varying model of COVID-19 pandemic exploiting basis functions, Biomed Signal Process Control 70 (2021) 102999, doi:10.1016/j.bspc.2021.102999.

[2] H. Akaike, A new look at the statistical model identification, IEEE transactions on automatic control 19 (6) (1974) 716–723.

[3] H. Akaike, Information theory and an extension of the maximum likelihood principle, in: Selected papers of hirotugu akaike, Springer, 1998, pp. 199–213.

[4] K. Asahi, E.A. Undurraga, R. Wagner, Benchmarking the COVID-19 pandemic across countries and states in the USA under heterogeneous testing, Scientific Reports 11 (1) (2021) 1–11.

[5] A.L. Bertozzi, E. Franco, G. Mohler, M.B. Short, D. Sledge, The challenges of modeling and forecasting the spread of covid-19, Proceedings of the National Academy of Sciences 117 (29) (2020) 16732–16738.

[6] A. Borri, P. Palumbo, F. Papa, C. Possieri, Optimal design of lock-down and re-opening policies for early-stage epidemics through SIR-D model, Annual Reviews in Control (2020), doi:10.1016/j.arcontrol.2020.12.002.
[7] A. Bousquet, W.H. Conrad, S.O. Sadat, N. Vardanyan, Y. Hong, Deep learning forecasting using time-varying parameters of the SIRD model for Covid-19, Scientific Reports 12 (1) (2022) 3030.
[8] C. Buzzi, M. Tucci, R. Ciprandi, I. Brambilla, S. Caimmi, G. Ciprandi, G.L. Marseglia, The psycho-social effects of COVID-19 on Italian adolescents' attitudes and behaviors, Italian Journal of Pediatrics 46 (69) (2020) 1–7.
[9] G.C. Calafiore, C. Novara, C. Possieri, A time-varying sird model for the covid-19 contagion in italy, Annual Reviews in Control 50 (2020) 361–372, doi:10.1016/j.arcontrol.2020.10.005.
[10] E.F. Camacho, C.B. Alba, Model predictive control, Springer science & business media, 2013.
[11] R. Carli, G. Cavone, N. Epicoco, P. Scarabaggio, M. Dotoli, Model predictive control to mitigate the COVID-19 outbreak in a multi-region scenario, Annual Reviews in Control (2020).
[12] F. Castanos, S. Mondié, Observer-based predictor for a susceptible-infectious-recovered model with delays: An optimal-control case study, International Journal of Robust and Nonlinear Control (2021), doi:10.1002/rnc.5522.
[13] P. Di Giamberardino, D. Iacoviello, F. Papa, C. Sinisgalli, Dynamical evolution of COVID-19 in Italy with an evaluation of the size of the asymptomatic infective population, IEEE J Biomed Health Inform 25 (2021) 1326–1332, doi:10.1109/JBHI.2020.3009038.
[14] Dipartimento della Protezione Civile, COVID-19 Italia - Monitoraggio della situazione, GitHub, 2020. https://github.com/pcm-dpc/COVID-19/tree/master/dati-andamento-nazionale
[15] Effectiveness of non-pharmaceutical interventions on COVID-19 transmission in 190 countries from 23 January to 13 April 2020, International Journal of Infectious Diseases 102 (2021) 247–253.
[16] D.M. Feehan, A.S. Mahmud, Quantifying population contact patterns in the United States during the COVID-19 pandemic, Nature communications 12 (1) (2021) 1–9.
[17] D. García-Violini, R. Sánchez-Peña, M. Moscoso-Vásquez, F. Garelli, Non-pharmaceutical intervention to reduce COVID-19 impact in Argentina, ISA Trans 124 (2022) 225–235, doi:10.1016/j.isatra.2021.06.024.
[18] M. Gatto, E. Bertuzzo, L. Mari, S. Miccoli, L. Carraro, R. Casagrandi, A. Rinaldo, Spread and dynamics of the COVID-19 epidemic in Italy: Effects of emergency containment measures, PNAS 117 (19) (2020) 10484–10491.
[19] X. Geng, G.G. Katul, F. Gerges, E. Bou-Zeid, H. Nassif, M.C. Boufadel, A kernel–modulated SIR model for COVID-19 contagious spread from county to continent, Proceedings of the National Academy of Sciences 118 (21) (2021).
[20] G. Giordano, F. Blanchini, R. Bruno, P. Colaneri, A.D. Filippo, A.D. Matteo, M. Colaneri, Modelling the COVID-19 epidemic and implementation of population-wide interventions in Italy, Nature Medicine 26 (2020) 855–860.
[21] G. Giordano, M. Colaneri, A. Di Filippo, F. Blanchini, P. Bolzern, G. De Nicolao, P. Sacchi, P. Colaneri, R. Bruno, Modeling vaccination rollouts, sars-cov-2 variants and the requirement for non-pharmaceutical interventions in italy, Nature Medicine (2021) 1–6.
[22] Google mobility reports, (https://www.google.com/covid19/mobility/). Accessed: 2021/12/06.
[23] M. Iannelli, A. Pugliese, Mathematical modeling of epidemics, Springer International Publishing, Cham, 2014, pp. 209–264.
[24] ISTAT, Intercensal population estimates. Demographic balance, Italian National Institute of Statistics, 2018. http://demo.istat.it/index.html
[25] J. Köhler L. Schwenkel, A. Koch, J. Berberich, P. Pauli, F. Allgöwer, Robust and optimal predictive control of the COVID-19 outbreak, 2020, (arXiv:2005.03580).
[26] W.O. Kermack, A.G. McKendrick, A contribution to the mathematical theory of epidemics, Proceedings of the royal society of London. Series A 115 (772) (1927) 700–721.
[27] L. Ljung, System identification, in: Signal analysis and prediction, Springer, 1998, pp. 163–173.
[28] A. Mandel, V. Veetil, The economic cost of COVID lockdowns: An out-of-equilibrium analysis, Economics of Disasters and Climate Change 4 (2020) 431–451.
[29] T.G. Molnár, A.W. Singletary, G. Orosz, A.D. Ames, Safety-critical control of compartmental epidemiological models with measurement delays, IEEE Control Systems Letters 5 (5) (2021) 1537–1542, doi:10.1109/LCSYS.2020.3040948.
[30] M.M. Morato, S.B. Bastos, D.O. Cajueiro, J.E. Normey-Rico, An optimal predictive control strategy for COVID-19 (SARS-CoV-2) social distancing policies in brazil, Annual Reviews in Control (2020).
[31] M.M. Morato, I. Pataro, M.A. da Costa, J. Normey-Rico, A parametrized nonlinear predictive control strategy for relaxing COVID-19 social distancing measures in Brazil, ISA Trans 124 (2022) 197–214, doi:10.1016/j.isatra.2020.12.012.
[32] M.M. Morato, G. dos Reis, J. Normey-Rico, A Sequential Quadratic Programming Approach for the Predictive Control of the COVID-19 Spread, IFAC-PapersOnLine 54 (15) (2021) 139-144, doi:10.1016/j.ifacol.2021.10.245.
[33] I.M.L. Pataro, M.M. Morato, M.V.A. da Costa, J.E. Normey-Rico, Optimal Control Approach for the COVID-19 Pandemic in Bahia and Santa Catarina, Brazil, Journal of Control, Automation and Electrical Systems 33 (1) (2022) 49–62.
[34] U. Patel, P. Malik, D. Mehta, D. Shah, R. Kelkar, C. Pinto, M. Suprun, M. Dhamoon, N. Hennig, H. Sacks, Early epidemiological indicators, outcomes, and interventions of COVID-19 pandemic: a systematic review, Journal of global health 10 (2) (2020).
[35] N. Perra, Non-pharmaceutical interventions during the COVID-19 pandemic: A review, Phys Rep 913 (2021) 1–52, doi:10.1016/j.physrep.2021.02.001.
[36] W.C. Roda, M.B. Varughese, D. Han, M.Y. Li, Why is it difficult to accurately predict the covid-19 epidemic? Infectious Disease Modelling 5 (2020) 271–281.
[37] V. Saladino, D. Algeri, V. Auriemma, The psychological and social impact of COVID-19: New perspectives of well-being, Frontiers in Psychology 11 (2020) 1–6.
[38] P. Scarabaggio, R. Carli, G. Cavone, N. Epicoco, M. Dotoli, Non-Pharmaceutical Stochastic Optimal Control Strategies to Mitigate the COVID-19 Spread, IEEE Transactions on Automation Science and Engineering (2021) 49–62, doi:10.1109/TASE.2021.3111338.
[39] A. Spelta, A. Flori, F. Pierri, G. Bonaccorsi, F. Pammoli, After the lockdown: simulating mobility, public health and economic recovery scenarios, Nature 10 (2020) 1–13.
[40] World Health Organization (WHO), Coronavirus Disease (COVID-19) Dashboard, (https://www.who.int/data1-dashboards).